

Danggui Buxue Decoction Attenuates H₂O₂-Induced HaCaT Cells by Modulating SOD2 Antioxidant and P21 Senescence Pathways

Xingyu Chen¹, Huilan Zheng², Hongbin Cheng¹, Jingping Wu², Gang Wang³, Ming Liu⁴,
Qianqian Yang², Qingjing Yang¹

¹Department of Dermatology, Hospital of Chengdu University of Traditional Chinese Medicine, Chengdu University of Traditional Chinese Medicine, Chengdu, Sichuan, 610075, People's Republic of China; ²Department of Medical Cosmetology, Hospital of Chengdu University of Traditional Chinese Medicine, Chengdu, Sichuan, 610075, People's Republic of China; ³National Engineering Research Center for Biomaterials, College of Biomedical Engineering, Sichuan University, Chengdu, Sichuan, 610064, People's Republic of China; ⁴Department of Medical Oncology/Gastric Cancer Center, West China Hospital, Sichuan University, Chengdu, Sichuan, 610075, People's Republic of China

Correspondence: Hongbin Cheng, Department of Dermatology, Hospital of Chengdu University of Traditional Chinese Medicine, Chengdu University of Traditional Chinese Medicine, Chengdu, Sichuan, 610075, People's Republic of China, Email chenghongbin@cduetcm.edu.cn; Jingping Wu, Department of Medical Cosmetology, Hospital of Chengdu University of Traditional Chinese Medicine, Chengdu, Sichuan, 610075, People's Republic of China, Email wujingping@cduetcm.edu.cn

Background: Skin aging is linked to oxidative stress, and functional decline of keratinocytes is a core feature. Common chemical anti-aging agents, such as retinoic acid, often cause skin irritation, whereas traditional Chinese medicine formulas, with multiple components and relatively low toxicity, may offer alternative strategies.

Methods: To investigate its antiaging effects and mechanisms, an in vitro oxidative stress model was established using H₂O₂-treated human HaCaT cells. The cellular safety of Danggui Buxue Decoction was assessed by CCK-8 assay and cell morphology. The effects of pretreatment on cell viability, intracellular reactive oxygen species, superoxide dismutase and glutathione peroxidase activities, and malondialdehyde content were evaluated. Real-time quantitative PCR was used to determine the mRNA expression of senescence- and oxidative stress-related genes.

Results: Exposure to 600 μmol/L H₂O₂ for 1 h established an oxidative stress model, reducing cell viability to 66.3%, increasing ROS and MDA levels, and decreasing SOD and GSH-Px activities. Danggui Buxue Decoction showed no cytotoxicity at 6.25–1600 μg/mL. Pretreatment with 400 μg/mL Danggui Buxue Decoction provided protection against oxidative damage, improving cell viability, lowering ROS and MDA levels, and restoring SOD and GSH-Px activities. Specifically, 400 μg/mL Danggui Buxue Decoction increased cell viability by 31.7%, enhanced SOD and GSH-Px activities by 91.3% and 32.2%, respectively, and reduced MDA content by 27.9%. Gene expression analysis indicated that pretreatment prevented the H₂O₂-induced decrease in SOD2 and MMP1 expression and attenuated the H₂O₂-induced overexpression of PPARα and P21.

Conclusion: Danggui Buxue Decoction exerts preventive antiaging protective effects on HaCaT cells by scavenging excess reactive oxygen species, preventing impairment of the endogenous antioxidant enzyme system, inhibiting lipid peroxidation, and regulating key genes such as SOD2, MMP1, PPARα, and P21, thereby interrupting the vicious cycle of oxidative stress-induced cellular senescence and supporting its potential as a natural anti-aging agent. In vivo and clinical studies are needed to validate the translational applicability of these findings in the future.

Keywords: skin aging, Danggui Buxue Decoction, oxidative stress, antioxidation, cellular senescence

Introduction

Skin aging is a progressive pathological process resulting from the combined effects of intrinsic aging and extrinsic environmental stimuli (such as ultraviolet radiation and air pollution). It manifests not only as increased wrinkles, reduced elasticity, and pigmentation but also as impaired epidermal barrier function and immune dysregulation, thereby increasing the risk of degenerative diseases such as atopic dermatitis and xerosis cutis.¹ Among the various mechanisms

regulating skin aging, oxidative stress is widely recognized as a core driving factor. Under physiological conditions, intracellular reactive oxygen species (ROS) act as signaling molecules involved in processes such as proliferation and differentiation, with their production and clearance maintaining a dynamic balance. However, with aging or intensified exogenous stimuli, excessive ROS accumulation surpasses the threshold of endogenous antioxidant defenses, triggering a series of damaging reactions, including DNA damage, protein oxidation, and lipid peroxidation, ultimately inducing functional decline in keratinocytes.²

Keratinocytes are the primary functional cells of the epidermis and constitute approximately 90% of the total epidermal cells. Their proliferative capacity and differentiation status directly determine epidermal thickness and barrier integrity. HaCaT cells, a commonly used cell line derived from human keratinocytes, are often employed in skin research. Their proliferative capacity and differentiation status directly determine epidermal thickness and barrier integrity. When HaCaT cells are subjected to oxidative stress damage, they exhibit senescent phenotypes, such as proliferation inhibition, increased apoptosis, and reduced antioxidant enzyme activity, leading to slowed epidermal renewal rates and diminished barrier repair capabilities. This is the key pathological basis for the “thinning epidermis, dryness, and sensitivity” observed in skin aging.³ Currently, the hydrogen peroxide (H₂O₂)-induced oxidative stress model in HaCaT cells is widely used as an in vitro tool for studying skin aging. H₂O₂, as an exogenous ROS donor, can simulate core pathological changes in natural aging through dose-dependent mechanisms, offering advantages such as operational simplicity, high model stability, and strong reproducibility.^{4,5} Existing studies have confirmed that treatment with appropriate concentrations of H₂O₂ induces typical aging characteristics in HaCaT cells, such as decreased cell viability, a rounded morphology, and enlarged intercellular gaps, accompanied by reduced activity of endogenous antioxidant enzymes (eg superoxide dismutase (SOD) and glutathione peroxidase (GSH-Px)) and the accumulation of lipid peroxidation end products (malondialdehyde (MDA)). These changes strongly align with the oxidative stress microenvironment of in vivo skin aging,⁶ providing a reliable experimental platform for evaluating the effects and mechanisms of anti-aging substances.

In the traditional Chinese medicine system, the core pathogenesis of skin aging is defined as “deficiency of qi and blood”. An imbalance of qi and blood synergy can lead to “dull skin and wrinkles”.⁷ On the basis of this theory, Danggui Buxue Decoction (DBD), as a classic compound formula for “tonifying qi and nourishing blood”, is composed of *Angelica sinensis* and *Astragalus membranaceus* in a 1:5 ratio. It was first recorded in Li Dongyuan’s “Treatise on Differentiation of Internal and External Injuries” during the Jin Dynasty and has been clinically applied for more than 800 years. It is typically used to improve skin dryness, salt complexion, and lack of luster caused by qi and blood deficiency.⁸ Recent pharmacological studies have confirmed that the core active components of this formula possess independent antioxidant potential: *Astragalus polysaccharides* from *Astragalus membranaceus* can activate AMPK/mTOR signaling to promote autophagy and increase cellular ROS clearance capacity;⁹ astragaloside IV can upregulate SOD1 and GPX1 gene expression, increasing antioxidant enzyme synthesis levels;¹⁰ and angelica polysaccharides from *Angelica sinensis* can reduce ROS-mediated DNA damage;¹¹ while ferulic acid directly quenches free radicals by providing hydrogen atoms.¹² Among natural antioxidants investigated for skin anti-aging, curcumin has shown protective effects against UV-induced skin damage,⁵ while soybean isoflavones demonstrate antiphotaging properties.⁶ However, most studies focus on single compounds or individual plant extracts. In contrast, Danggui Buxue Decoction (DBD), as a classical compound formula containing multiple bioactive components from two complementary herbs, offers potential advantages through multi-component, multi-target synergistic effects for more comprehensive regulation of the oxidative stress-cellular senescence axis. Recent studies have also highlighted the significant effects of DBD in diseases related to oxidative stress. In a lung cancer mouse model, which exhibits high levels of oxidative stress, DBD delayed tumor growth by inhibiting HIF-1 α /VEGF-mediated angiogenesis. This further demonstrates the multi-target regulatory effects of DBD in oxidative stress-related diseases, including cancer.¹³ However, research on the effects of DBD in HaCaT cell oxidative stress models remains limited. Key questions, particularly regarding how the multicomponent formula regulates oxidative stress and aging and whether it functions through repairing the antioxidant enzyme system and inhibiting lipid peroxidation pathways, have not yet been answered. Additionally, the use of commonly used synthetic chemical ingredients in the field of skin anti-aging (such as retinol and retinoids), while showing certain anti-aging effects, is often accompanied by adverse reactions such as skin irritation and photosensitivity. Long-term use may disrupt skin microenvironment homeostasis.^{14,15} In contrast, traditional Chinese medicine compounds, which are based on the

concept of “holistic regulation”, offer the advantages of multiple components, multiple targets, and low toxicity and better align with the clinical demand for “safe and effective” skin anti-aging preparations.

Therefore, in this study, an oxidative stress-induced senescence model in HaCaT cells was established using H₂O₂. First, pre-experiments were conducted to optimize the H₂O₂ concentration and safe dosage range of DBD. Subsequently, by evaluating cell viability, ROS levels, antioxidant enzyme activity, and MDA content, the antiaging protective effects of DBD were systematically evaluated. Finally, the molecular mechanism were elucidated from the perspective of “scavenging ROS, restoring antioxidant enzymes, and inhibiting lipid peroxidation”. This study aims to provide modern experimental evidence for the effects of DBD on skin aging and to offer new directions for the development of natural antiaging formulations based on traditional Chinese medicine.

Materials and Methods

Reagents and Instruments

Reagents: DBD (Affiliated Hospital of Chengdu University of Traditional Chinese Medicine, lyophilized powder, Chengdu, Sichuan, China; 5.45 g of raw herb per 1 g of lyophilized powder); 30% hydrogen peroxide (Chengdu Jinshan Chemical Reagent Co., Ltd., Chengdu, Sichuan, China; no batch number); Penicillin–Streptomycin solution (Beijing Solarbio Science & Technology Co., Ltd., Beijing, China; batch number P1400); CCK-8 kit (Beijing Solarbio Science & Technology Co., Ltd., Beijing, China; batch number CA1210); Reactive Oxygen Species (ROS) detection kit (Beijing Solarbio Science & Technology Co., Ltd., Beijing, China; batch number CA1410); Superoxide Dismutase (SOD) activity detection kit (Beijing Solarbio Science & Technology Co., Ltd., Beijing, China; batch number BC5165); Glutathione Peroxidase (GSH-Px) activity detection kit (Beijing Solarbio Science & Technology Co., Ltd., Beijing, China; batch number BC1195); Malondialdehyde (MDA) content detection kit (Beijing Solarbio Science & Technology Co., Ltd., Beijing, China; batch number BC6415); 0.22 µm disposable syringe filters (Biosharp, Hefei, Anhui, China; batch number BS-PES25-22-S); DMEM high-glucose medium (Beijing Solarbio Science & Technology Co., Ltd., Beijing, China).

Cell Culture

Human immortalized keratinocyte HaCaT cells were purchased from Beina Biology Technology Co., Ltd. The cells were cultured in complete medium (containing 89% high-glucose DMEM, 10% fetal bovine serum, and 1% penicillin–streptomycin) at 37 °C and 5% CO₂. Cells were seeded at a density of 1 × 10⁵/mL, and their morphology and growth status were regularly observed under an inverted optical microscope. When the cells reached 80–90% confluence, they were subcultured. Cells from passages 8–10 with good growth status were selected for experiments.

To establish the oxidative stress model, HaCaT cells in good condition were seeded and cultured until they reached 60–70% confluence, after which the medium of the control group was replaced with serum-free medium and cultured for 25 h; the H₂O₂ model group was cultured in serum-free medium for 24 h and then treated with 600 µmol/L H₂O₂ for 1 h, and the DBD pretreatment group was first pretreated with serum-free medium supplemented with 400 µg/mL DBD for 24 h, followed by treatment with 600 µmol/L H₂O₂ for 1 h.

Effects of DBD on HaCaT Cell Growth

Freeze-dried powder from Danggui Buxue Decoction was dissolved in PBS to prepare a 10 mg/mL stock solution. It was ultrasonically dissolved under an ice bath at 200 W (3 s per cycle, 10s intervals, 30 cycles total), followed by sterilization through filtration using a 0.22 µm sterile syringe filter. The stock solution was sequentially diluted with complete DMEM to prepare drug-containing working solutions with low concentrations (6.25–400 µg/mL) and high concentrations (50–6400 µg/mL). HaCaT cells were seeded into 96-well plates (100 µL/well) and 6-well plates (2 mL/well) and cultured until they reached 60–70% confluency, after which the original medium was discarded. Different concentrations of drug-containing culture medium were added, and the cells were incubated for 24 h. After treatment, 100 µL of CCK-8 working solution was added to each well of the 96-well plate, followed by incubation at 37 °C and 5% CO₂ in the dark

for 1 h. The OD value at 450 nm was measured to calculate cell viability. Simultaneously, the 6-well plates were observed under an optical microscope to assess morphological changes and evaluate potential drug toxicity.

Establishment of the H₂O₂-Induced Oxidative Stress Model

Thirty percent H₂O₂ (9.8 mol/L) was prepared fresh and sequentially diluted into a 1 mol/L stock solution and a 10 mmol/L intermediate stock solution. These solutions were then diluted with complete culture medium to prepare six working concentrations ranging from 100–1000 μmol/L. Cells were seeded as described above and cultured until they reached 60–70% confluence. The culture medium was discarded, and the cells were treated with different concentrations of H₂O₂ solutions for 1 h. After treatment, the H₂O₂-containing medium was removed, and the cells were gently washed three times with PBS. Cell viability was measured using the CCK-8 assay, and morphological features such as cell shrinkage, changes in the intercellular gap, and refractivity were observed. On the basis of the combined cell morphology and survival rate results, 600 μmol/L H₂O₂ was ultimately determined to be the optimal concentration.

Detection of Cell Viability (CCK-8 Assay)

Cell viability was determined using the CCK-8 assay. In brief, HaCaT cells were seeded in 96-well plates at a density of 100 μL per well and cultured until the cell confluence reached 60%–70%. Afterward, the cells were pretreated with media containing 400, 800, or 1600 μg/mL DBD for 24 h. The drug-containing medium was discarded, and the cells were gently washed with PBS three times, followed by treatment with 600 μmol/L H₂O₂ for 1 h. After the intervention, 100 μL of CCK-8 working solution was added to each well, and the plates were incubated in the dark at 37 °C with 5% CO₂ for 1 h. The absorbance of each well was measured at 450 nm using a microplate reader, and the cell survival rate was calculated according to the following formula: Cell survival rate (%) = [(OD value of experimental group – OD value of blank well) / (OD value of control group – OD value of blank well)] × 100%. The blank well contains complete culture medium with CCK-8 reagent but without cells, serving to correct for background absorbance.

Intracellular Reactive Oxygen Species (ROS) Assay

The logarithmically growing HaCaT cells were seeded in 6-well plates at a density of 1 × 10⁵ cells/mL (2 mL complete medium per well). The cells were cultured at 37 °C with 5% CO₂ until they reached approximately 80% confluence. Drug intervention and modeling were performed according to the grouping method described in Section *Cell Culture*. After intervention, the original medium was discarded, and 1 mL of 10 μmol/L DCFH-DA working solution prepared in serum-free DMEM was added to each well to ensure complete coverage of the cells. The cells were incubated at 37 °C with 5% CO₂ in the dark for 20 min to allow sufficient probe entry into the cells. After incubation, the probe-containing medium was aspirated, and the cells were gently washed three times with prewarmed serum-free DMEM (5 min each time) to remove residual probes that did not enter the cells. The cells were observed under an inverted fluorescence microscope, and green fluorescence (DCF) images were captured. ImageJ software was used to quantitatively analyze the fluorescence intensity, which reflects the level of intracellular ROS.

SOD Activity, GSH-Px Activity, and MDA Content Detection

Cells were seeded in 6-well plates (2 mL/well) as described above. After the interventions were performed, the medium was discarded, and the cells were washed twice with precooled 1 × PBS (1 mL each time). The cells were collected, resuspended in 200 μL of PBS, and subjected to ultrasonic lysis (300 W power, 3-s sonication, 30-s intervals, repeated 3 times). The samples were subsequently centrifuged at 4 °C and 2000 × g for 10 min, after which the supernatant was collected for subsequent measurements.

SOD activity was measured strictly according to the instructions of the Superoxide Dismutase Assay Kit (Solarbio, batch number BC5165), and the absorbance was detected at a wavelength of 450 nm to calculate enzyme activity. GSH-Px activity was determined with a Glutathione Peroxidase Assay Kit (Solarbio, batch number BC1195), and the absorbance value was read at a wavelength of 412 nm to calculate the enzyme activity. The MDA content was measured according to the instructions of the Malondialdehyde Assay Kit (Solarbio, batch number BC6415), the OD532 and

OD600 values were determined to calculate the MDA content, and the MDA concentration was calculated according to the formula provided in the instructions.

RNA Extraction and Real-Time Fluorescence Quantitative PCR (RT–qPCR)

HaCaT cells were seeded into 6-well plates (2 mL/well) according to the aforementioned method and subjected to drug pretreatment and H₂O₂ modeling intervention. Total RNA was extracted from the cells using a kit method, followed by removal of genomic DNA and reverse transcription to synthesize cDNA using the PrimeScript™ RT Reagent Kit with gDNA Eraser. β -actin was used as the internal reference gene, and real-time fluorescent quantitative PCR amplification was performed using the TB Green® Premix Ex Taq™ II kit. The RT–qPCR program was set as follows: predenaturation at 95 °C for 30s; denaturation at 95 °C for 5 s; and annealing and extension at 60 °C for 30s for a total of 45 cycles. The sequences of primers used for detecting the expression of target genes were as follows:

β -actin:

F: GAAGGTGACAGCAGTCGGTT

R: GGGACTTCCTGTAACAACGCA

SOD2:

F: CCCAGCAAGATAATGTCCTGTC

R: AATGCAGACCTCTTTGATGGTT

MMP1:

F: AGGGGAGATCATCGGGACAA

R: GCATCCCCTCCAATACCTGG

PPAR α :

F: GAAAAGGCTATACGGACCACC

R: TTTGTTGCCCTCAGCACAGT

P21:

F: TCTTGTACCCTTGTGCCTCG

R: TGGTAGAAATCTGTCATGCTGGT

Relative quantitative analysis of target gene mRNA expression was performed using the comparative Ct (Δ Ct) method by normalizing the Ct values of the target genes to the Ct values of the internal reference gene β -actin.

Statistical Analysis

Data statistics and graph plotting were conducted using GraphPad Prism 10.1 software. Measurement data are expressed as the mean \pm standard deviation (mean \pm standard deviation); prior to intergroup comparisons, the Shapiro–Wilk test was used for normality analysis, and the Brown–Forsythe test was used for homogeneity of variance analysis. For intergroup comparisons, when normality and homogeneity of variance were satisfied ($P > 0.05$ for both tests), one-way analysis of variance (ANOVA) was applied, with Tukey’s honestly significant difference test for pairwise comparisons. If either normality or homogeneity of variance was not met ($P < 0.05$ for either test), the non-parametric Kruskal–Wallis rank sum test was used, with Dunn’s method for pairwise comparisons. All experiments were performed independently at least three times ($n \geq 3$), and $P < 0.05$ was considered to indicate statistical significance.

Results

Effects of H₂O₂ on HaCaT Cell Viability and Morphology

To establish an oxidative stress model, HaCaT cells were treated with different concentrations of H₂O₂ (100–1000 μ mol/L) for 1 h, after which changes in cell viability and morphology were detected. Compared with those in the control group, cell survival rates significantly decreased in a concentration-dependent manner with increasing H₂O₂ concentration ($P < 0.05$) (Figure 1A). Specifically, the cell survival rates in the 400, 600, and 800 μ mol/L groups decreased to $78.2 \pm 5.1\%$, $66.3 \pm 4.7\%$, and $49.0 \pm 5.5\%$, respectively. Morphological observations further confirmed this trend (Figure 1B): cells maintained a normal morphology after low-dose (100–200 μ mol/L) treatment; mild shrinkage was observed in the 400 μ mol/L group; the 600 μ mol/L group

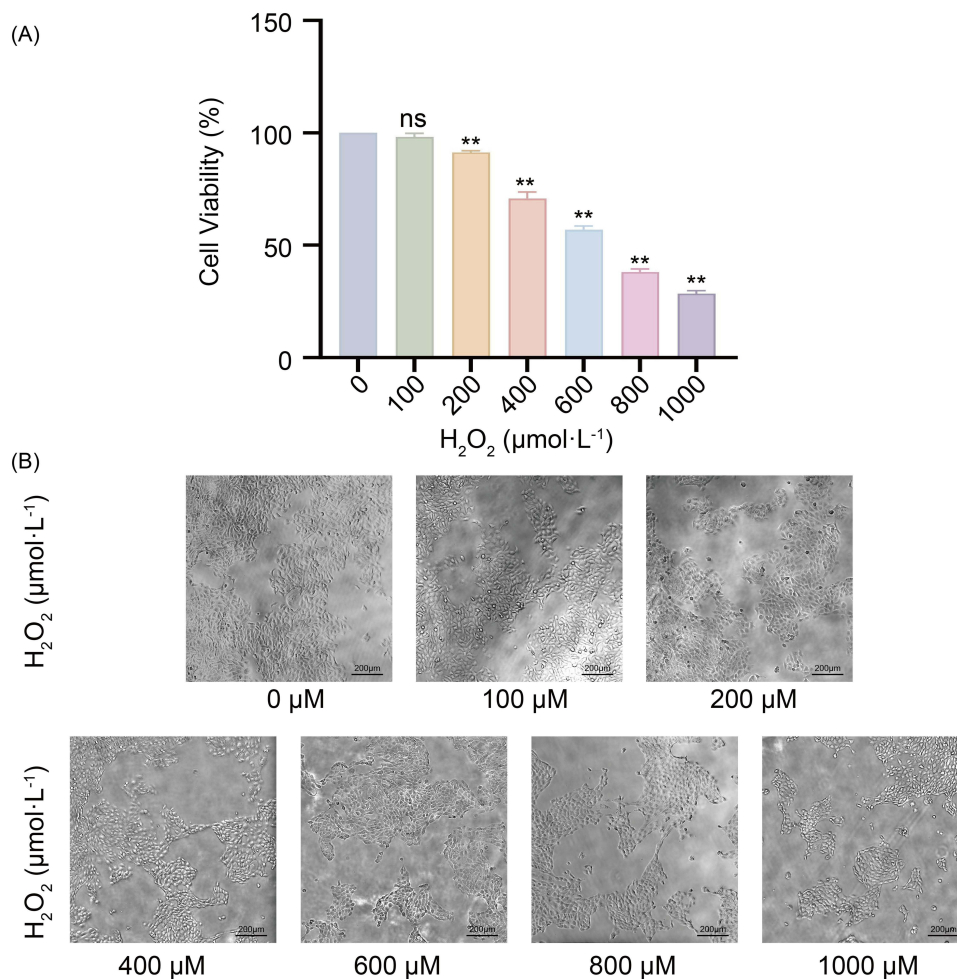


Figure 1 Effects of H₂O₂ on HaCaT cell viability and morphological changes under oxidative stress. **(A)** Cell viability after treatment with different concentrations of H₂O₂. ns, not significant; ** $P < 0.01$ compared with the 0 μmol/L group. **(B)** Changes in the morphology of HaCaT cells after treatment with different concentrations of H₂O₂. The data are presented as the means \pm standard deviations (SD), $n = 3$.

exhibited typical oxidative stress characteristics (increased gaps, rounded cells, and enhanced refractivity) while retaining a large number of viable cells; and the 800 μmol/L group showed significant detachment and extensive cell death. On the basis of the combined analysis of cell viability and morphology, 600 μmol/L H₂O₂ was selected as the optimal treatment condition for subsequent oxidative stress models, as it ensured stable induction of damage while retaining a detectable number of cells.

Effects of DBD on the Viability and Morphology of HaCaT Cells

To evaluate the toxicity of DBD on HaCaT cells, the cells were treated with a concentration gradient of 6.25–6400 μg/mL for 24 h. The results (Figure 2A) revealed that within the range of 6.25–1600 μg/mL, there was no significant difference in cell viability compared with that of the control group ($P > 0.05$), which maintained a range of 90%–110%. Only at 3200 μg/mL did cell viability significantly decrease ($P < 0.05$). The morphological results (Figure 2B) further indicated that the cells in the 50–1600 μg/mL treatment groups adhered normally, exhibited a plump morphology, and showed no obvious shrinkage or detachment. These results suggest that DBD has no significant cytotoxicity within the experimental dose range needed. In subsequent experiments, 400, 800, and 1600 μg/mL were selected as the intervention doses.

Protective Effect of DBD on H₂O₂-Induced HaCaT Cell Injury

To investigate the protective effect of DBD, HaCaT cells were pretreated with different doses (400–1600 μg/mL) for 24 h before H₂O₂ treatment. The cell viability results (Figure 3A) revealed that the survival rate of the model group (600 μmol/L H₂O₂)

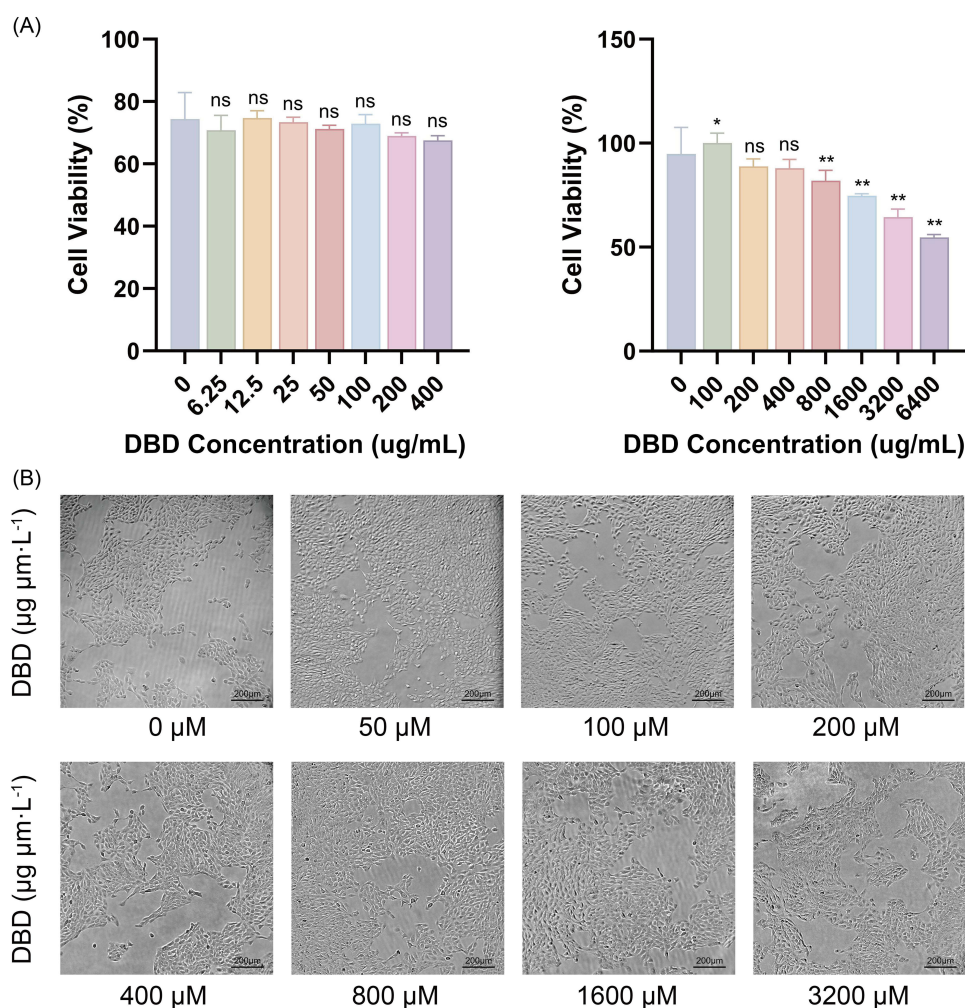


Figure 2 Effects of DBD on HaCaT cell viability and morphology. **(A)** HaCaT cell viability after treatment with different concentrations of DBD. **(B)** Changes in the morphology of HaCaT cells treated with different concentrations of DBD. ns, not significant; * $P < 0.05$, ** $P < 0.01$ compared with the 0 μM group. The data are presented as the means \pm standard deviations (SD), $n = 3$.

significantly decreased to $56.4 \pm 6.7\%$ ($P < 0.05$), confirming the successful establishment of the oxidative stress model. Compared with the model group, all the groups treated with DBD had significantly increased cell viability ($P < 0.05$); the survival rates of the 400 $\mu\text{g}/\text{mL}$, 800 $\mu\text{g}/\text{mL}$, and 1600 $\mu\text{g}/\text{mL}$ groups increased by 31.7%, 28.9%, and 31.7%, respectively. Among them, the 400 $\mu\text{g}/\text{mL}$ group exhibited more stable protective effects and the smallest standard deviation; thus, it was selected as the optimal dose for subsequent mechanistic studies.

Effects of DBD on H_2O_2 -Induced ROS Generation

ROS levels were detected using a DCFH-DA fluorescent probe. The results (Figure 3B and C) revealed that H_2O_2 treatment significantly increased intracellular ROS levels ($248.6 \pm 19.8\%$, $P < 0.001$), with the fluorescence intensity markedly greater than that in the control group ($100.0 \pm 10.4\%$). However, after pretreatment with 400 $\mu\text{g}/\text{mL}$ DBD, H_2O_2 -induced ROS accumulation was significantly reduced to $152.1 \pm 14.0\%$ ($P < 0.001$). These findings indicate that DBD effectively reduces the generation of ROS caused by oxidative stress.

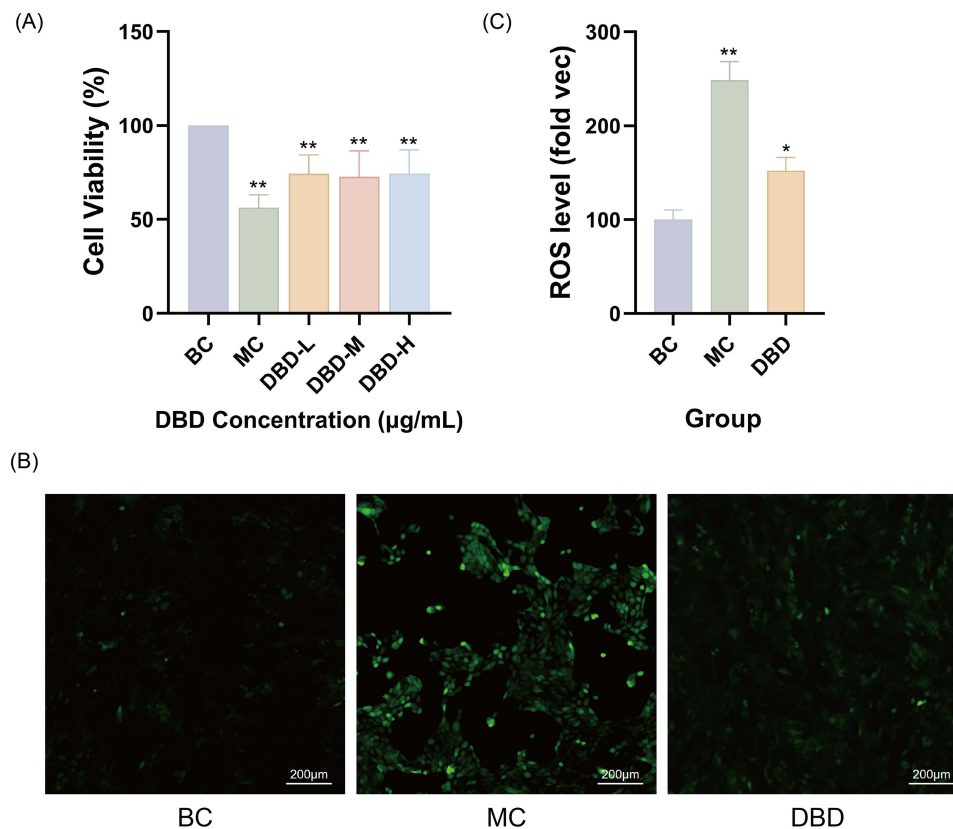


Figure 3 Protective effects of DBD against H_2O_2 -induced oxidative damage in HaCaT cells. **(A)** DBD pretreatment prevented the decrease of cell viability in a dose-dependent manner in HaCaT cells exposed to H_2O_2 . **(B)** Representative fluorescence microscopy images showing intracellular ROS levels detected by the DCFH-DA probe. Scale bar = 100 µm. **(C)** Quantitative analysis of the relative ROS fluorescence intensity from fluorescence microscopy images. BC, blank control group; MC, model group; DBD, 400 µg/mL DBD; DBD-L, M, H means 400, 800 and 1600 µg/mL DBD respectively. * $P < 0.05$, ** $P < 0.01$ compared with the blank control group. The data are presented as the means \pm standard deviations (SD), $n = 3$.

Effects of DBD on SOD and GSH-Px Activities and MDA Contents in H_2O_2 -Induced HaCaT Cells

Further detection of endogenous antioxidant enzymes and lipid peroxidation levels was performed (Figure 4). Compared with those in the control group, the SOD activity in the model group decreased by 59.6%, the GSH-Px activity decreased by 29.7%, and the MDA content increased by 8.7% (all $P < 0.05$), indicating an impaired antioxidant system.

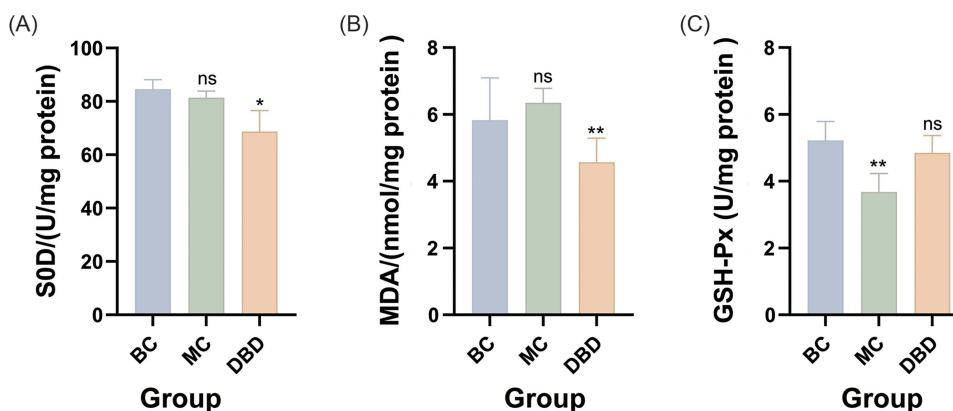


Figure 4 Effects of DBD on antioxidant enzyme activity and lipid peroxidation in H_2O_2 -induced HaCaT cells. **(A)** Superoxide dismutase (SOD) activity. **(B)** Malondialdehyde (MDA) content. **(C)** Glutathione peroxidase (GSH-Px) activity. BC, blank control group; MC, model group; DBD, 400 µg/mL DBD. ns, not significant; * $P < 0.05$, ** $P < 0.01$ compared with the blank control group. The data are presented as the means \pm standard deviations (SD), $n = 3$.

Pretreatment with DBD significantly improved these indicators ($P < 0.05$): the activity of SOD increased by 91.3%, the activity of GSH-Px increased by 32.2%, and the content of MDA decreased by 27.9%. These results suggest that DBD can restore cellular antioxidant defense function by increasing antioxidant enzyme activity and reducing lipid peroxidation.

Regulatory Effects of DBD on Oxidative Stress and the Expression of Genes Related to Cellular Senescence

To further explore the molecular mechanism through which DBD protects against oxidative stress and premature aging, this study examined the mRNA expression levels of genes related to antioxidant capacity, matrix metabolism, lipid metabolism regulation, and the cell cycle (SOD2, MMP1, PPAR α , and P21) in HaCaT cells.

As shown in Figure 5, compared with the blank control group (BC), H₂O₂ stimulation significantly altered the expression patterns of the aforementioned genes: the mRNA expression of the antioxidant-related gene SOD2 was significantly downregulated to approximately 0.57 times that of the control group ($P < 0.05$), and the expression of the matrix metabolism-related gene MMP1 also decreased to approximately 0.55 times ($P < 0.05$). Moreover, the expression levels of the metabolic/transcriptional regulatory factor PPAR α and the cell cycle inhibitory protein P21 significantly

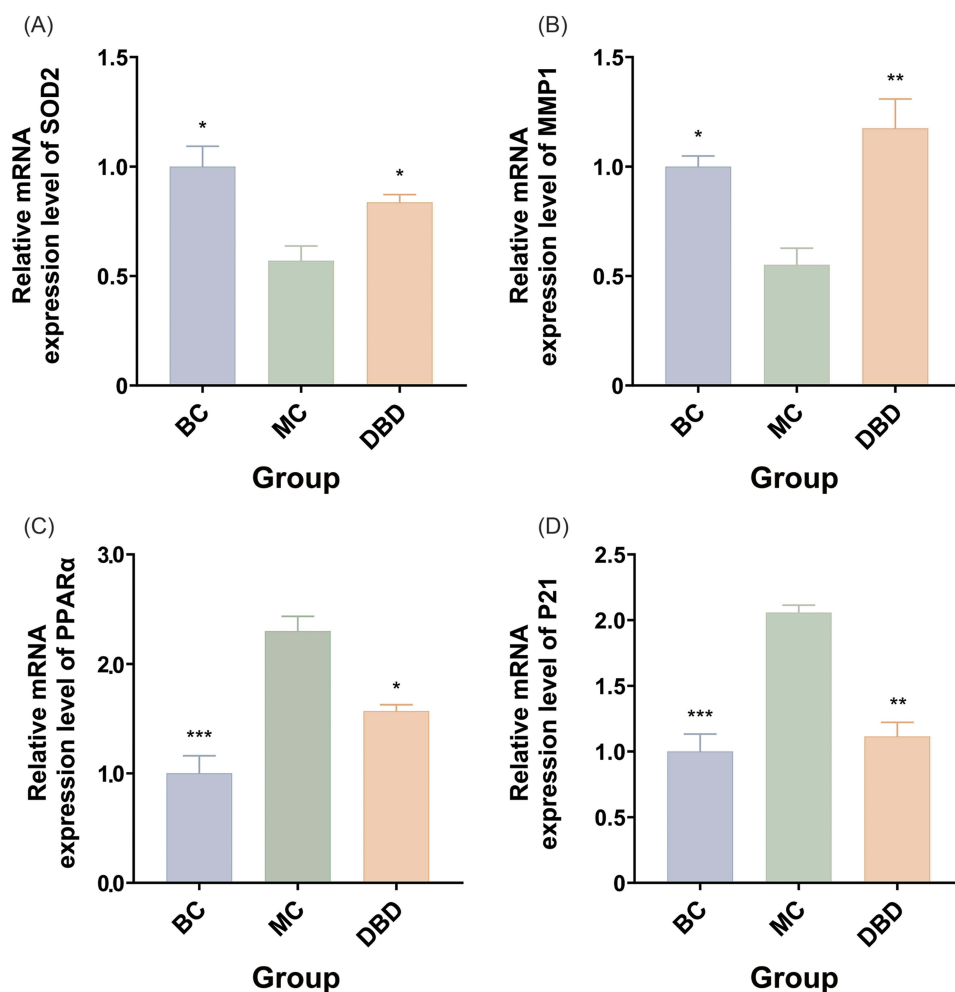


Figure 5 Effects of DBD on the mRNA expression of genes related to oxidative stress and senescence in H₂O₂-induced HaCaT cells. (A) Relative mRNA expression level of SOD2. (B) Relative mRNA expression level of MMP1. (C) Relative mRNA expression level of PPAR α . (D) Relative mRNA expression level of P21. BC, blank control group; MC, model group; DBD, 400 μ g/mL DBD. * $P < 0.05$, ** $P < 0.01$, *** $P < 0.001$ compared with the Model group (H₂O₂ only). The data are presented as the means \pm standard deviations (SD), $n = 3$.

increased (approximately 2.30 times and 2.06 times that of the control group, respectively; $P < 0.01$). These changes suggest that H_2O_2 successfully induced oxidative stress and premature aging in HaCaT cells.

Pretreatment with DBD significantly reversed these abnormal expression trends. Compared with those in the model group (MC), the expression of both SOD2 and MMP1 significantly increased in the DBD pretreatment group (Group D) (approximately 1.47-fold and 2.13-fold that in the model group, respectively; $P < 0.05$), whereas the mRNA levels of PPAR α and P21 significantly decreased (to approximately 0.68-fold and 0.54-fold those in the model group, respectively; $P < 0.05$). Further comparisons revealed that there were no significant differences in the expression of SOD2, MMP1, or P21 between the DBD group and the control group ($P > 0.05$), indicating that their expression largely returned to normal levels. PPAR α in the DBD group remained slightly greater than that in the control group (approximately 1.57-fold), but the difference was only close to significance ($P \approx 0.057$). All the data underwent appropriate statistical testing, and except for PPAR α (comparison between Group D and the control group), the other pairwise comparisons revealed significant differences ($P < 0.05$).

These results indicate that H_2O_2 can induce typical oxidative stress and changes in the expression of genes related to premature senescence in HaCaT cells, whereas DBD can effectively inhibit this process. The underlying mechanisms may include the upregulation of antioxidant genes such as SOD2, the restoration of normal MMP1 expression, and the suppression of abnormal activation of PPAR α and P21. Overall, DBD significantly alleviated H_2O_2 -induced oxidative damage and premature senescence. The direction of gene expression changes aligns with the previously observed results on cell viability, ROS levels, and antioxidant enzyme activities, further validating at the transcriptional level its cytoprotective effects through modulation of the “oxidative stress–cellular senescence” pathway.

Discussion

Skin aging is a complex biological process influenced by both intrinsic and extrinsic factors, and oxidative stress-induced cellular damage is considered the initiating factor of aging and persists throughout the aging process. Particularly in the epidermal layer, keratinocytes are the first cell type to be exposed to oxidative stress. When keratinocytes are affected by factors such as ultraviolet radiation, pollutants, and metabolic imbalances, their antioxidant capacity decreases, and cell cycle dysregulation occurs, thereby accelerating skin deterioration. In this study, an H_2O_2 -induced oxidative stress model was used to systematically analyze the regulatory effects of DBD on oxidative damage, the antioxidant enzyme system, lipid peroxidation, gene expression, and metabolic stress. The results demonstrate that DBD significantly protects against oxidative stress through synergistic multitarget and multipathway effects, helps restore cellular homeostasis, and effectively inhibits the aging process. These findings establish an experimental foundation for its modern application in the field of skin antiaging.

Systemic Regulation of the Antioxidant Pathway: SOD–SOD2–GSH-Px–MDA

Oxidative stress has been demonstrated to be among the core driving factors in the process of skin aging. Both endogenous metabolic disorders and exogenous factors such as ultraviolet radiation, environmental pollution, and unhealthy lifestyle habits can ultimately promote the excessive generation of ROS. Excessive ROS can damage DNA, protein, and lipid structures and induce inflammatory responses and signaling imbalances, thereby forming a vicious cycle of “oxidative damage—cellular senescence”.¹ Under normal circumstances, cells maintain redox balance through the activity of antioxidant enzymes such as SOD, SOD2, and GSH-Px. However, when the intensity of H_2O_2 stimulation exceeds the defense threshold, the oxidative chain becomes imbalanced, leading to excessive free radical production, a decline in mitochondrial antioxidant capacity, and ineffective clearance of peroxides, ultimately exacerbating lipid peroxidation. In this study, the ROS levels in the model group significantly increased, whereas the activities of SOD and GSH-Px decreased to 40.4% and 70.3% of those in the control group, respectively. SOD2 mRNA expression was significantly suppressed, and the level of MDA increased by 8.7%, indicating that the antioxidant system was markedly impaired. This damage trend aligns with the patterns observed in previous oxidative stress research.³ These changes are highly consistent with alterations in oxidative indicators during human aging.¹⁶ Thus, the SOD–SOD2–GSH-Px–MDA antioxidant chain not only determines the immediate survival capacity of keratinocytes under stress but is also closely related to long-term structural damage and functional degeneration.

Among them, SOD2 is a key enzyme involved in maintaining oxidative homeostasis. SOD2 is located within the mitochondria and is responsible for clearing superoxide anions (O_2^-). A decrease in SOD2 leads to the accumulation of ROS in mitochondria, which in turn disrupts membrane potential and inhibits respiratory chain activity, forming a vicious cycle of “ROS–mitochondrial damage–more ROS”.^{17–21} In this study, the SOD2 mRNA level in the H_2O_2 model group decreased to approximately 0.57 times that in the control group, which is highly consistent with the decrease in total SOD activity, the increase in ROS, and the accumulation of MDA, indicating that the mitochondrial antioxidant defense system is among the most severely damaged parts. These findings align with those of previous studies in which SOD2-deficient mice exhibited significant aging phenotypes and excessive mitochondrial ROS accumulation,^{20,21} further demonstrating that this model successfully recapitulates the oxidative stress-dominated premature aging state. The most critical effect of DBD in this study is the systematic repair of the aforementioned antioxidant pathways. Compared with those in the model group, the activity of SOD increased significantly (91.3%), the activity of GSH-Px increased (32.2%), the activity of MDA decreased (27.9%), and the activity of SOD2 mRNA expression significantly recovered. This finding not only indicates the restoration of primary ROS clearance capacity but also suggests enhanced H_2O_2 processing ability, reestablishment of the mitochondrial antioxidant barrier, and inhibition of lipid peroxidation terminal steps. Such comprehensive improvement from the initial stage to the final stage cannot be achieved by conventional single antioxidants, aligning more with the characteristics of traditional Chinese medicine compounds that restore overall balance through multicomponent and multitarget synergistic effects. The synergistic recovery of SOD2 and GSH-Px is particularly crucial in this process, as they jointly regulate mitochondrial ROS levels: SOD2 is responsible for clearing superoxide anions, while the latter (GSH-Px) removes the H_2O_2 generated by their disproportionation. An imbalance between the two leads to aggravated oxidative damage.²² The ability of DBD to simultaneously restore both steps indicates that its antioxidant effects are not limited to a single reaction pathway but involve the regulation of multiple related nodes in the antioxidant process.

On the other hand, the decrease in MDA also indicated that oxidative damage was ameliorated at the structural level. As a typical end product of lipid peroxidation, MDA not only serves as an indicator of membrane structural damage but also reacts with proteins and nucleic acids, exacerbating the aging process.²³ In this study, the MDA level increased in the model group, whereas under the intervention of DBD, the MDA level significantly decreased, indicating that the decoction not only inhibited the oxidative stress cascade but also effectively blocked the occurrence of structural damage. More importantly, a decline in SOD activity accompanied by elevated MDA levels is a significant predictor of increased all-cause mortality risk in elderly individuals.²⁴ Therefore, the improvement in the activity of SOD–MDA in combination with DBD is important not only at the cellular level but also for its long-term antiaging potential.

Overall, the role of DBD in the antioxidant pathway manifests as reducing ROS accumulation, restoring SOD/SOD2 and GSH-Px activity, and inhibiting MDA production, thereby restoring the entire oxidative cascade from an imbalanced state to normal equilibrium. This systemic regulatory pattern aligns with modern antioxidant theories, resonates with the traditional concept of “supporting vital qi and consolidating the foundation”, and is highly consistent with the practical applications of SOD-like substances in skin protection.²⁵ This study provides the first cellular-level evidence demonstrating that DBD can reconstruct the antioxidant network, offering robust mechanistic support for its role as a natural antiaging intervention.

Regulation of Matrix Balance and Metabolic Stress: MMP1 and PPAR α

During the process of cell damage induced by oxidative stress, the matrix renewal mechanisms and energy metabolism status are also critical factors determining the maintenance of epidermal homeostasis. Unlike the antioxidant system, matrix renewal and energy metabolism more directly influence cell structure and metabolism and can more sensitively reflect the cell’s repair or decline status. The results of this study demonstrated that both MMP1 and PPAR α exhibited significant abnormal changes under H_2O_2 stimulation, whereas intervention with DBD restored both to levels closer to those associated with physiological homeostasis, providing strong evidence for understanding its antiaging mechanisms.

MMP1 is the primary enzyme responsible for the degradation of type I and III collagen and plays a physiological role in promoting extracellular matrix (ECM) turnover during normal skin renewal. In general, MMP1 is often upregulated in photoaging models or chronic inflammatory conditions, leading to accelerated ECM degradation and resulting in skin

wrinkles and loss of elasticity. However, under acute oxidative stress conditions (such as H₂O₂ stimulation), cells do not exhibit this pattern of excessive ECM degradation but instead tend to suppress MMP1 to minimize additional structural damage. Previous studies have indicated that under acute injury, cells tend to enter a “protective ECM suppression state”, temporarily reducing matrix metabolism to conserve resources and limit structural damage.^{26–30} In this study, the significant decrease in MMP1 in the model group aligns completely with this acute stress protective mechanisms.

Importantly, DBD does not forcibly increase the expression of MMP1 but rather prevents it from being strongly inhibited by H₂O₂ to a level close to normal. These findings indicate that DBD does not act by “promoting matrix degradation” or “inhibiting degradation” but by ameliorating upstream damage stress, thereby restoring the rhythm of ECM renewal. This physiological regulatory approach is highly consistent with the holistic adjustment characteristics of compound formulations. This compound not only alters the expression of a single target gene but also, by alleviating oxidative stress and improving the cellular environment, enables cells to regain their normal ability to regulate the ECM. This approach aligns more closely with the principles of tissue repair than merely inhibiting or promoting MMP1. In other words, the role of DBD is not to drive ECM degradation but to restore the stable state of the ECM, which also explains why it is traditionally regarded in medical theory as having the function of “nourishing blood and moisturizing the skin”.

In addition, the changes in PPAR α reflect the imbalance of cellular energy metabolism under oxidative stress. PPAR α is a key regulator of the fatty acid β -oxidation pathway, and its upregulation typically occurs when cells face high energy demands, impaired repair stress, or increased oxidative pressure; thus, it is regarded as a marker of cellular metabolic stress. Under oxidative stimulation, cells compensate by activating PPAR α activity to adapt to metabolic instability. However, sustained metabolic stress can push cells into a state of excessive stress, leading to increased mitochondrial ROS production and thereby exacerbating oxidative damage. In this study, a significant increase in the PPAR α after H₂O₂ stimulation indicated that the cells were in a “high metabolic stress mode”, corroborated by elevated ROS levels, mitochondrial damage, and decreased GSH-Px activity. Notably, the high activation of PPAR α signifies that cells have reached their energy compensation limit. If stress is not alleviated, accelerated aging or programmed cell death may ensue.

After intervention with DBD, the expression of PPAR α significantly decreased to near-normal levels, indicating that by reducing oxidative stress and improving mitochondrial antioxidant capacity, cells no longer need to rely on compensatory metabolic stress to maintain basic functions. This mode of action suggests that DBD prevents the decrease in metabolic homeostasis by “removing stress sources” rather than simply inhibiting the PPAR α metabolic pathway. From a cell biology perspective, compared with directly targeting PPAR α , improving the overall cellular environment and allowing spontaneous return to normal states aligns more closely with the logic of natural cellular repair.

Comprehensive analysis revealed that changes in the expression of MMP1 and PPAR α indicate that oxidative stress not only disrupts antioxidant pathways but also interferes with ECM renewal and energy metabolism. By restoring these two aspects, DBD helps cells revert to normal regulatory patterns in both dimensions, preventing excessive suppression of the ECM and alleviating metabolic stress. This dual restorative effect prevents structural damage while improving metabolic functionality, establishing a robust mechanistic foundation for its antiaging efficacy.

P21-Mediated Senescence Fate Programming and the Reversal Mechanism of DBD

P21 (CDKN1A), a cell cycle inhibitory protein, serves as a central hub connecting the DNA damage response (DDR) with the senescence program. Its expression level directly determines whether cells enter repair or senescence after oxidative stress. Numerous studies have shown that P21 is rapidly activated following DNA damage, inhibiting the ability of CDK2 to arrest cells in the G1/S or G2/M phase, thereby providing time for genome repair.³¹ This mechanism is crucial for maintaining genomic stability. However, if damage persists or cannot be effectively repaired, sustained upregulation of P21 drives cells into irreversible senescent arrest, resulting in the formation of the typical “p53–P21–RB” senescence axis, which is among the common patterns in skin photoaging and intrinsic aging.³² In this study, H₂O₂ stimulation led to significant upregulation of P21 expression, which is consistent with the classical biological response in which ROS induce DNA damage and activate the p53 pathway under oxidative stress conditions.^{33–37}

However, an increase in P21 does not necessarily mean that it should be inhibited. P21 acts as a double-edged sword: a moderate elevation aids in DNA repair, but sustained high expression indicates that the cell has entered an irreversible senescent state. Therefore, high levels of P21 are often regarded as biomarkers of cumulative damage, with its elevation

reflecting the cell's transition from "reversible arrest" to "irreversible senescence". This finding also implies that any intervention capable of substantially alleviating upstream oxidative stress, improving mitochondrial function, and reducing lipid peroxidation may indirectly lower P21 by decreasing DNA damage pressure. This constitutes a "reasonable P21 downregulation" rather than mere simple inhibition.

The findings of this study align with this mechanism. After intervention with DBD, the expression of P21 significantly decreased and tended toward physiological levels. This finding is highly consistent with evidence such as the reduction in ROS, restoration of SOD/SOD2, increased activity of GSH-Px, and downregulation of MDA, indicating that its mechanism of action does not directly interfere with cell cycle molecules. Instead, it increases oxidative stress pathways, prevents impairment mitochondrial damage, and alleviates metabolic burdens, thereby eliminating the need for cells to maintain high levels of P21 to block the cell cycle. This "natural downregulation of P21" achieved by mitigating upstream damage aligns with the view proposed in cutting-edge research that "P21 function depends on its molecular stability, protein interactions, and duration of sustained expression".³⁸ In other words, the effect of DBD more closely resembles the autonomous recovery of the cell cycle after "stress relief" rather than drugs forcibly promoting cell proliferation. This is key to ensuring normal cellular renewal capacity and long-term safety.

Notably, the regulation of P21 not only affects cell cycle arrest but is also closely related to the rhythm of epidermal differentiation and renewal during skin aging. Studies have shown that in keratinocytes, excessive P21 can inhibit normal differentiation and weaken epidermal barrier construction by regulating the IGF-I-related pathway.³⁹ Combined with the observed downward trend of P21 in this study, it can be speculated that DBD, in addition to improving cycle arrest, may also have beneficial effects on the physiological differentiation process of keratinocytes, thereby supporting its theoretical basis in traditional medical principles of "nourishing blood, moisturizing the skin, and improving skin texture".

Overall, the P21 regulatory results revealed in this study indicate that DBD reduces oxidative damage and metabolic stress, allowing cells to recover from abnormal defensive states and causing P21 expression to decrease from "stress-induced overexpression" to normal levels, thereby effectively blocking the premature initiation of the aging program. This finding not only demonstrates its antioxidant effects but also highlights its profound effect on cell fate regulation. These comprehensive results suggest that DBD can help cells overcome the vicious cycle of "damage—arrest—senescence", restore normal proliferation, differentiation, and repair functions, and provide strong molecular mechanism support for its potential as a natural anti-aging agent.

DBD involves the construction of a comprehensive protective network that spans "oxidative stress—metabolic stress—structural homeostasis—aging regulation" through the systematic regulation of the antioxidant pathway (SOD—SOD2—GSH-Px—MDA), the restoration of ECM and metabolic homeostasis (MMP1 and PPAR α), and the blockade of the senescence fate program (P21). Its mode of action fully reflects the advantages of traditional Chinese medicine compound formulations in multitarget and multipathway synergistic regulation, providing a solid molecular mechanism foundation for its role as a natural antiaging intervention.

Notably, the pretreatment design employed here demonstrates DBD's preventive and protective effects against oxidative stress-induced senescence, not restorative effects on pre-existing damage. Future studies using post-treatment designs (inducing damage first, then administering DBD) would be needed to evaluate potential therapeutic effects on already-damaged cells. This study was conducted in an in vitro H₂O₂-induced oxidative stress model using immortalized HaCaT cells, which may not fully reflect the complexity of normal human skin in vivo. The doses was selected based on preliminary toxicity screening and literature precedent; however, exploring a broader concentration range in future studies may identify additional effective doses. Only a limited concentration range of Danggui Buxue Decoction was evaluated, and no in vivo or long-term studies were performed, so its systemic effects, chronic safety, and sustained efficacy remain to be determined in the future. While we measured MMP1 mRNA expression as a validated biomarker of ECM metabolism, direct evaluation of ECM structural and functional changes—such as collagen content quantification, procollagen synthesis assessment, ECM integrity visualization, and mechanical property measurements—was not performed in this study due to the current constraints. Future investigations should incorporate complementary assays including hydroxyproline quantification, procollagen type I C-peptide (PIP) ELISA, and immunofluorescence staining for collagen fibers to comprehensively assess the protective effects of DBD on skin matrix homeostasis. Therefore, further animal and clinical studies are needed to validate these findings and extend their translational relevance.

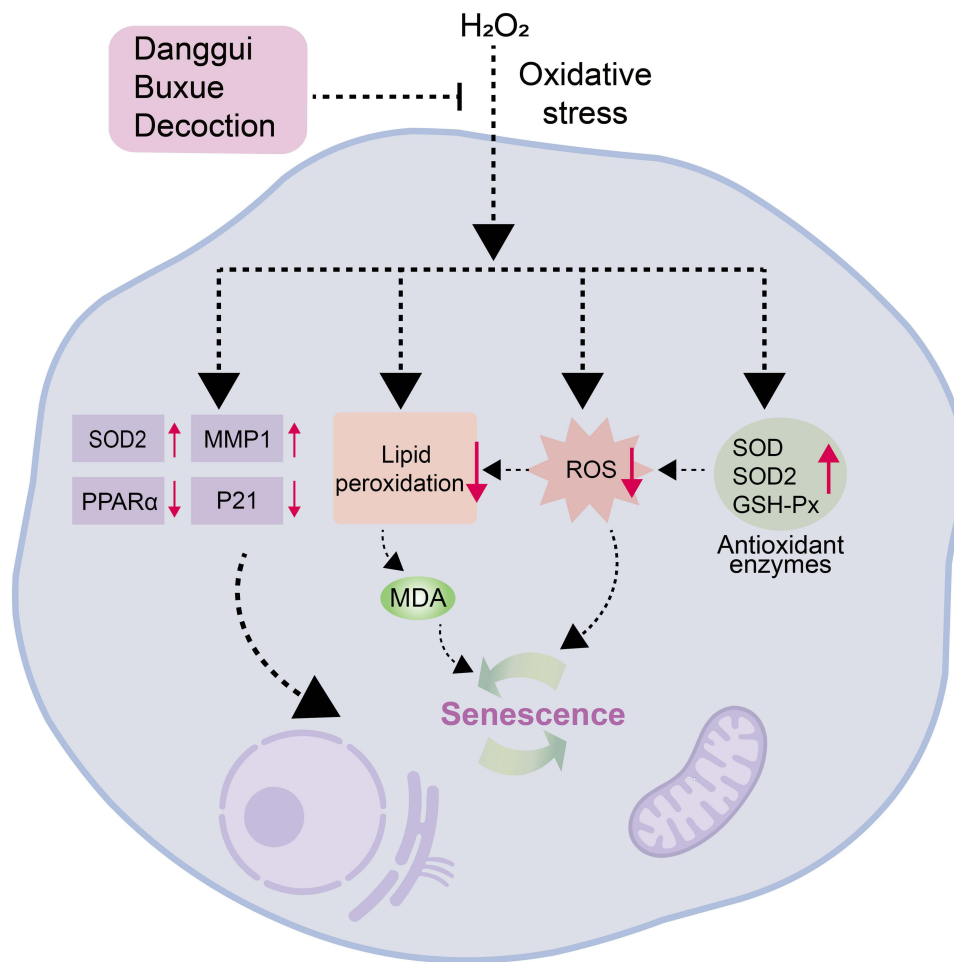


Figure 6 Mechanism of Danggui Buxue Decoction (DBD) protecting HaCaT cells from H₂O₂-induced oxidative stress and senescence. Red upward arrows (↑) indicate upregulation or increased levels; red downward arrows (↓) indicate downregulation or decreased levels.

Conclusion

This study confirmed that Danggui Buxue Decoction (DBD) effectively protects HaCaT keratinocytes from H₂O₂-induced oxidative stress and cellular senescence. The protective mechanisms include the clearance of excess ROS, enhancement of SOD and GSH-Px activity, inhibition of lipid peroxidation by reducing MDA levels, and modulation of key genes such as SOD2, MMP1, PPAR α , and P21. By regulating these genes, DBD breaks the oxidative stress-induced cellular senescence cycle, thus slowing down the aging process. Furthermore, this study lays the foundation for future research into how Danggui Buxue Decoction attenuates H₂O₂-induced cell damage through the modulation of the SOD2 antioxidant pathway and P21 senescence pathway (Figure 6). This provides new directions for exploring its potential in anti-aging and skin health promotion. The experimental findings support the use of Danggui Buxue Decoction as a natural therapeutic strategy for preventing skin aging.

Abbreviations

TGF- β , Transforming Growth Factor-beta; SOD, Superoxide Dismutase; GSH-Px, Glutathione Peroxidase; MDA, Malondialdehyde; AMPK, Activated Protein Kinase; mTOR, Mechanistic Target of Rapamycin; SOD2, Superoxide Dismutase 2; MMP1, Matrix Metalloproteinase 1; PPAR α , Peroxisome Proliferator-Activated Receptor Alpha; P21, Cyclin-Dependent Kinase Inhibitor 1A.

Data Sharing Statement

The original contributions presented in the study are included in the article, further inquiries and requests for data can be directed to the corresponding author Jingping Wu (wujingping@cducm.edu.cn).

Author Contributions

All authors made a significant contribution to the work reported, whether that is in the conception, study design, execution, acquisition of data, analysis and interpretation, or in all these areas; took part in drafting, revising or critically reviewing the article; gave final approval of the version to be published; have agreed on the journal to which the article has been submitted; and agree to be accountable for all aspects of the work.

Funding

This work was supported by the Registration and Development of Seven-Ingredient Itch-Relieving Powder as a Traditional Chinese Medicine Preparation for Medical Institutions (Grant No. 2024zd037); Development and Application of Astragalus and Coptis Formula for Melasma Treatment (Grant No. 2024zd022); Clinical Efficacy and Mechanism of Action of the Umbilical Eight-Point Acupuncture Method in Treating Simple Obesity with Spleen Deficiency and Dampness Accumulation (Grant No. 2024MS317); Efficacy, Safety, and Mechanism Evaluation of Yufu Cream in Treating Mild to Moderate Atopic Dermatitis in Adults (Grant No. 2024MS318); Registration and Development of Xiao Bang Gao as a Traditional Chinese Medicine Preparation for Medical Institutions (Grant No. 25ZDIZX022); and Exploring the Regulation of Fibroblast Senescence by Sanhuang Zengmian Decoction in the Treatment of Melasma with Deficiency of Qi and Yin via the SCF/c-kit/MAPK Signaling Pathway (Grant No. 2024YFFK0165).

Disclosure

The authors report no conflicts of interest in this work.

References

- Shen CY, Jiang JG, Yang L, Wang DW, Zhu W. Anti-ageing active ingredients from herbs and nutraceuticals used in traditional Chinese medicine: pharmacological mechanisms and implications for drug discovery. *Br J Pharmacol.* 2017;174(11):1395–1425. doi:10.1111/bph.13631
- Ma SX, Lee PC, Jiang I, et al. Influence of age, gender and race on nitric oxide release over acupuncture points-meridians. *Sci Rep.* 2015;5(1):17547. doi:10.1038/srep17547
- Michalak M. Plant-derived antioxidants: significance in skin health and the ageing process. *Int J Mol Sci.* 2022;23(2):585. doi:10.3390/ijms23020585
- Lee YR, Noh EM, Kwon KB, et al. Radix clematidis extract inhibits UVB-induced MMP expression by suppressing the NF-kappaB pathway in human dermal fibroblasts. *Int J Mol Med.* 2009;23(5):679–684. doi:10.3892/ijmm_00000180
- Sumiyoshi M, Kimura Y. Effects of a turmeric extract (*Curcuma longa*) on chronic ultraviolet B irradiation-induced skin damage in melanin-possessing hairless mice. *Phytomedicine.* 2009;16(12):1137–1143. doi:10.1016/j.phymed.2009.06.003
- Chiu TM, Huang CC, Lin TJ, et al. In vitro and in vivo anti-photoaging effects of an isoflavone extract from soybean cake. *J Ethnopharmacol.* 2009;126(1):108–113. doi:10.1016/j.jep.2009.07.039
- Zhu S, Jia L, Wang X, et al. Anti-aging formula protects skin from oxidative stress-induced senescence through the inhibition of CXCR2 expression. *J Ethnopharmacol.* 2024;318(Pt B):116996. doi:10.1016/j.jep.2023.116996
- Qian H, Shan Y, Gong R, et al. Mechanism of action and therapeutic effects of oxidative stress and stem cell-based materials in skin aging: current evidence and future perspectives. *Front Bioeng Biotechnol.* 2022;10:1082403. doi:10.3389/fbioe.2022.1082403
- Ichijo R, Maki K, Kabata M, et al. Vasculature atrophy causes a stiffened microenvironment that augments epidermal stem cell differentiation in aged skin. *Nat Aging.* 2022;2(7):592–600. doi:10.1038/s43587-022-00244-6
- Liu T, Xia Q, Lv Y, et al. ErZhiFormula prevents UV-induced skin photoaging by Nrf2/HO-1/NQO1 signaling: an in vitro and in vivo studies. *J Ethnopharmacol.* 2023;309:115935. doi:10.1016/j.jep.2022.115935
- Chajra H, Salwinski A, Guillaumin A, et al. Plant milking technology-an innovative and sustainable process to produce highly active extracts from plant roots. *Molecules.* 2020;25(18):4162. doi:10.3390/molecules25184162
- Tian LM, Xie HF, Xiao X, et al. Study on the roles of β -catenin in hydrogen peroxide-induced senescence in human skin fibroblasts. *Exp Dermatol.* 2011;20(10):836–838. doi:10.1111/j.1600-0625.2011.01324.x
- Chen W, Guo Y, Liu H, et al. Danggui Buxue decoction attenuates 4-(methylnitrosamino)-1-(3-pyridyl)-1-butanone-induced lung cancer growth in A/J mice by suppressing HIF-1 α /VEGF-mediated angiogenesis. *Front Med.* 2025;12:1687685. doi:10.3389/fmed.2025.1687685
- He XL, Wang N, Teng X, et al. Dendrobium officinale flowers' topical extracts improve skin oxidative stress and aging. *J Cosmet Dermatol.* 2024;23(5):1891–1904. doi:10.1111/jocd.16210

15. Zagórska Dziok M, Mokrzyńska A, Ziemlewska A, et al. Assessment of the antioxidant and photoprotective properties of *Cornus mas* L. Extracts on HDF, hacat and a375 cells exposed to uva radiation. *Int J Mol Sci.* 2024;25(20):10993. doi:10.3390/ijms252010993
16. Pandey KB, Rizvi SI. Markers of oxidative stress in erythrocytes and plasma during aging in humans. *Oxid Med Cell Longev.* 2010;3(1):2–12. doi:10.4161/oxim.3.1.10476
17. Holley AK, Bakthavatchalu V, Velez-Roman JM, St Clair DK. Manganese superoxide dismutase: guardian of the powerhouse. *Int J Mol Sci.* 2011;12(10):7114–7162. doi:10.3390/ijms12107114
18. Miriyala S, Spasojevic I, Tovmasyan A, et al. Manganese superoxide dismutase, MnSOD and its mimics. *Biochim Biophys Acta.* 2012;1822(5):794–814. doi:10.1016/j.bbadis.2011.12.002
19. Azadmanesh J, Borgstahl GEO. A review of the catalytic mechanism of human manganese superoxide dismutase. *Antioxidants.* 2018;7(2):25. doi:10.3390/antiox7020025
20. Treiber N, Maity P, Singh K, et al. The role of manganese superoxide dismutase in skin aging. *Derm-Endocrinol.* 2012;4(3):232–235. doi:10.4161/derm.21819
21. Velarde MC, Flynn JM, Day NU, Melov S, Campisi J. Mitochondrial oxidative stress caused by Sod2 deficiency promotes cellular senescence and aging phenotypes in the skin. *Aging.* 2012;4(1):3–12. doi:10.18632/aging.100423
22. Ekoue DN, He C, Diamond AM, Bonini MG. Manganese superoxide dismutase and glutathione peroxidase-1 contribute to the rise and fall of mitochondrial reactive oxygen species which drive oncogenesis. *Biochim Biophys Acta Bioenergy.* 2017;1858(8):628–632. doi:10.1016/j.bbabi.2017.01.006
23. Cordiano R, Di Gioacchino M, Mangifesta R, et al. Malondialdehyde as a potential oxidative stress marker for allergy-oriented diseases: an update. *Molecules.* 2023;28(16):5979. doi:10.3390/molecules28165979
24. Mao C, Yuan JQ, Lv YB, et al. Associations between superoxide dismutase, malondialdehyde and all-cause mortality in older adults: a community-based cohort study. *BMC Geriatr.* 2019;19(1):104. doi:10.1186/s12877-019-1109-z
25. Zheng M, Liu Y, Zhang G, et al. The applications and mechanisms of superoxide dismutase in medicine, food, and cosmetics. *Antioxidants.* 2023;12(9):1675. doi:10.3390/antiox12091675
26. Xia W, Hammerberg C, Li Y, et al. Expression of catalytically active matrix metalloproteinase-1 in dermal fibroblasts induces collagen fragmentation and functional alterations that resemble aged human skin. *Aging Cell.* 2013;12(4):661–671. doi:10.1111/ace1.12089
27. Lee YH, Seo EK, Lee ST. Skullcapflavone II inhibits degradation of type I collagen by suppressing MMP-1 transcription in human skin fibroblasts. *Int J Mol Sci.* 2019;20(11):2734. doi:10.3390/ijms20112734
28. Lu J, Guo JH, Tu XL, et al. Tiron inhibits UVB-induced AP-1 binding sites transcriptional activation on MMP-1 and MMP-3 promoters by MAPK signaling pathway in human dermal fibroblasts. *PLoS One.* 2016;11(8):e0159998. doi:10.1371/journal.pone.0159998
29. Oh S, Park S, Lee P, Kim YM. The ginsenoside Rg2 downregulates MMP-1 expression in keratinocyte (HaCaT)-conditioned medium-treated human fibroblasts (Hs68). *Appl Biol Chem.* 2023;66(1):85. doi:10.1186/s13765-023-00843-w
30. Kim HH, Shin CM, Park CH, et al. Eicosapentaenoic acid inhibits UV-induced MMP-1 expression in human dermal fibroblasts. *J Lipid Res.* 2005;46(8):1712–1720. doi:10.1194/jlr.M500105-JLR200
31. Karimian A, Ahmadi Y, Yousefi B. Multiple functions of p21 in cell cycle, apoptosis and transcriptional regulation after DNA damage. *DNA Repair.* 2016;42:63–71. doi:10.1016/j.dnarep.2016.04.008
32. Engeland K. Cell cycle regulation: p53-p21-RB signaling. *Cell Death Differ.* 2022;29(5):946–960. doi:10.1038/s41418-022-00988-z
33. Al Bitar S, Gali Muhtasib H. The role of the cyclin dependent kinase inhibitor p21^{Cip1/Waf1} in targeting cancer: molecular mechanisms and novel therapeutics. *Cancers.* 2019;11(10):1475. doi:10.3390/cancers11101475
34. Dutto I, Tillhon M, Cazzalini O, Stivala LA, Prosperi E. Biology of the cell cycle inhibitor p21^{CDKN1A}: molecular mechanisms and relevance in chemical toxicology. *Arch Toxicol.* 2015;89(2):155–178. doi:10.1007/s00204-014-1430-4
35. Cazzalini O, Scovassi AI, Savio M, Stivala LA, Prosperi E. Multiple roles of the cell cycle inhibitor p21^{CDKN1A} in the DNA damage response. *Mutat Res Rev Mutat Res.* 2010;704(1–3):12–20. doi:10.1016/j.mrrev.2010.01.009
36. Hershenson MB. p21^{Waf1/Cip1} and the prevention of oxidative stress. *Am J Physiol Lung Cell Mol Physiol.* 2004;286(3):L502–L505. doi:10.1152/ajplung.00336.2003
37. Papismadov N, Gal H, Krizhanovsky V. The anti-aging promise of p21. *Cell Cycle.* 2017;16(21):1997–1998. doi:10.1080/15384101.2017.1377500
38. Ticali G, Cazzalini O, Stivala LA, Prosperi E. Revisiting the function of p21^{CDKN1A} in DNA repair: the influence of protein interactions and stability. *Int J Mol Sci.* 2022;23(13):7058. doi:10.3390/ijms23137058
39. Devgan V, Nguyen BC, Oh H, Dotto GP. p21^{WAF1/Cip1} suppresses keratinocyte differentiation independently of the cell cycle through transcriptional up-regulation of the IGF-1 gene. *J Biol Chem.* 2006;281(41):30463–30470. doi:10.1074/jbc.M604684200

Clinical, Cosmetic and Investigational Dermatology

Publish your work in this journal

Clinical, Cosmetic and Investigational Dermatology is an international, peer-reviewed, open access, online journal that focuses on the latest clinical and experimental research in all aspects of skin disease and cosmetic interventions. This journal is indexed on CAS. The manuscript management system is completely online and includes a very quick and fair peer-review system, which is all easy to use. Visit <http://www.dovepress.com/testimonials.php> to read real quotes from published authors.

Submit your manuscript here: <https://www.dovepress.com/clinical-cosmetic-and-investigational-dermatology-journal>

Dovepress
Taylor & Francis Group